Generation and measurement of velocity bunched ultrashort bunch of pC charge

X. H. Lu and C. X. Tang
Department of Engineering Physics, Tsinghua University, Beijing 100084, China

R. K. Li, H. To, G. Andonian, and P. Musumeci*
Department of Physics and Astronomy, UCLA, Los Angeles, California 90095, USA
(Received 6 August 2014; published 18 March 2015)

In this paper, we discuss the velocity compression in a short rf linac of an electron bunch from a rf photoinjector operated in the blowout regime. Particle tracking simulations shows that with a beam charge of 2 pC an ultrashort bunch duration of 16 fs can be obtained at a tight longitudinal focus downstream of the linac. A simplified coherent transition radiation (CTR) spectrum method is developed to enable the measurement of ultrashort (sub-50 fs) bunches at low bunch energy (5 MeV) and low bunch charges (<10 pC). In this method, the ratio of the radiation energy selected by two narrow bandwidth filters is used to estimate the bunch length. The contribution to the coherent form factor of the large transverse size of the bunch suppresses the radiation signal significantly and is included in the analysis. The experiment was performed at the UCLA Pegasus photoinjector laboratory. The measurement results show bunches of sub-40 fs with 2 pC of charge well consistent with the simulation using actual experimental conditions. These results open the way to the generation of ultrashort bunches with time-duration below 10 fs once some of the limitations of the setup (rf phase jitter, amplitude instability and low field in the gun limited by breakdown) are corrected.

DOI: 10.1103/PhysRevSTAB.18.032802 PACS numbers: 29.25.Bx, 06.30.Bp, 41.60.-m

I. INTRODUCTION

Ultrashort bunch lengths are demanded for several applications of high brightness electron beams including driving high gain free electron lasers (FEL) [1], high gradient laser and plasma based advanced accelerators [2], coherent generation of intense THz radiation [3] and ultrafast electron scattering sources [4,5].

In electron linacs, short bunches are typically obtained taking advantage of compression techniques where accelerating radio frequency (rf) fields are used to impart a velocity or energy chirp on the beam and then drift or dispersive sections are used to allow the faster particle in the beam tail to catch up with the slower particles in the front [6–8]. The final bunch length after compression is limited by a combination of effects including the longitudinal phase space area of the beam prior compression and the bunch charge. Due to the suppression of space charge effects when the particles are fully relativistic, ultrashort bunch lengths (sub-50 fs) have been obtained so far at high beam energies at the end of relatively long (tens of m) linacs.

*musumeci@physics.ucla.edu

In this paper we discuss a scheme where we aim at generating the shortest possible electron beam at low energy (<5 MeV) for application in ultrafast MeV electron diffraction setup [9–11]. Wang *et al.* discussed using the fields in the rf gun itself to compress the beam by launching the particle at a low injection phase [12]. Fukasawa *et al.* developed a novel rf structure, the hybrid gun [13,14], where the beam passes through a traveling wave section at a compressing phase. The issue in these cases is that in order for the compression to effectively work the beam has to be relatively long in the region where the rf fields impart the energy chirp. In practice, for pC-beam charges the compression only works if a ps-long laser pulse is used to illuminate the cathode with a corresponding increase in the longitudinal phase space emittance therefore setting a limit on the shortest attainable bunch lengths. In the scheme discussed here, we take advantage of the characteristic beam dynamics regime resulting from illuminating the cathode with an ultrashort laser pulse, commonly referred to as the blowout regime [15,16]. In this configuration, the beam expands under the action of the longitudinal space charge forces acquiring a linear correlation in longitudinal phase space. We then use a short high gradient rf linac to recompress it down to a sharp longitudinal focus [17].

In the experiment, a significant challenge in terms of longitudinal diagnostics was posed by the low beam charge and energy. For the low energy regime, the most widely employed method for bunch length measurement is using a time-varying transverse electrical field provided by a rf deflecting cavity to convert the longitudinal distribution into transverse coordinate [18,19]. This method is straightforward and robust but is not capable of capturing the locally compressed ultrashort bunch length in situations where bunch length changes significantly over distances shorter than the length of the cavity. The electro-optic method [20] can measure the bunch length within a short region (smaller than 1 mm), but it works best for highly relativistic beams and the temporal resolution is limited to 60 fs [21]. In the laser plasma acceleration field [2,22], as well as in the FEL community [1,23], spectral methods based on bunch-generated coherent transition radiation (CTR) are the most competitive candidates for the temporal characterization of bunch lengths shorter than 10 fs. These measurements are conventionally performed with scanning interferometer and yield the autocorrelation of the CTR signal [24,25]. Besides the use of an interferometer, single shot CTR spectrum retrieval method has been developed by Wesch *et al.*, using consecutive dispersion gratings and multichannel detector [26]. Several phase-retrieval algorithms can be used to reconstruct the longitudinal beam profile from the spectrum information [27,28]. In these measurement schemes, the bunch energy is typically over 50 MeV up to several GeV and the beam charge is larger than 50 pC [29], the radiation is emitted in a narrow cone and the CTR signal is intense (typically many μJ) and easily detectable.

Together with the novel beam dynamics, this paper discusses then a dedicated simplified CTR-based method developed specifically for measuring ultrashort bunch lengths for beams with low energy and low charge. The method exploits the strong enhancement of the high frequency components of the CTR spectrum when the bunch is fully compressed. In this method, two narrow-band filters at different frequencies are used to select the CTR energy in two separate spectral regions. Assuming a Gaussian longitudinal profile, then the ratio of the energies measured after the filters can be used to characterize the radiation spectrum and so yields an estimate for the bunch length. This method is particularly suitable for the diagnostic of measuring the ultrashort bunch length in ultrafast electron diffraction applications with rf compression schemes [30–32].

The paper is structured as follows. In Sec. II, we present the analysis of the beam line to generate the low charge, low energy ultrashort bunch using velocity bunching. In Sec. III, we calculate the CTR power emitted by the ultrashort beam, taking into consideration the large radiation emitting angle and the low beam energy, which jointly make the transverse coherence a significant factor in the measurement. For this reason, a solenoid is used to provide a small transverse beam size on the CTR target. In Sec. IV, we present the detection setup and the measurement procedure, as well as the discussion of the data. Finally, a summary is given in Sec. V.

II. GENERATION OF ULTRASHORT BUNCH BY VELOCITY BUNCHING

A. Basic scheme of velocity bunching

The generation of ultrashort bunch using an rf photogun operated in the blowout regime in conjunction with a velocity bunching linac for ultrafast MeV electron diffraction application has been proposed and previously discussed by Li *et al.* [32]. In that paper, it was shown that due to more efficient detectors, very low beam charges (still sufficient to acquire a single shot diffraction pattern) could be used for electron diffraction applications, thus offering a straightforward solution to the space-charge related limit in obtaining short electron bunches. Higher gradients inside rf gun also mitigate bunch lengthening by accelerating the electron into relativistic energy in a shorter period. Nevertheless, in order to obtain sub-30 fs bunch lengths with pC bunch charges a compression method must be applied.

The schematic of our setup for ultrashort bunch generation is shown in Fig. 1. The experiment has been carried out at the Pegasus advanced photoinjector laboratory at UCLA [16]. An S-band 1.6 cell photo cathode rf gun is used to generate relativistic electron bunch by illuminating the cathode with a 50 fs (rms) long laser pulse. In the blowout regime, the bunch develops a linear correlation in longitudinal phase space and the emittance growth is minimized [33]. A solenoid (solenoid A) after the rf gun focuses the bunch transversely, matching the transverse beam size into the velocity bunching linac. A 60 cm long S-band dual slot resonance linac (DSRL) operated at compressing phase (i.e., close to the zero crossing) is installed downstream, introducing a negative energy chirp (the beam tail gains more energy than the beam head). More details about the DSRL linac can be found in Ref. [34]. After a drift distance, the electrons at the tail catch up with the electrons at the head, and the shortest bunch length is achieved at a tight longitudinal focus. A target is located at the point of maximum compression. By tuning the field strength and the phase of linac, it is possible to control the position of longitudinal focus along the beam line. For example, by imparting larger energy chirps on the beam, the location of the maximum compression point moves closer to the linac.

We use the particle tracking code GPT [35] to simulate the velocity bunching process with the beam line layout

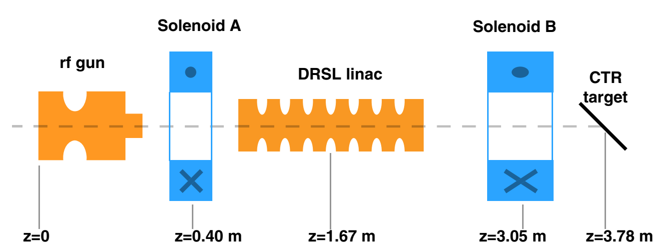

FIG. 1. Schematic of beam line for velocity bunching experiment (drawing not to scale).

described above. In these simulations, the gradient of the linac is set at the maximum value achievable with the available rf power and its phase is tuned to reach the longitudinal focus at different locations. The use of the solenoid B shown in Fig. 1 will be discussed in the later section of the paper. For the initial simulations discussed in this section it is turned off. Other parameters for the simulation are summarized in Table I. The gradient in the rf gun is limited by arcing to 70 MV/m and 25 degrees is the optimum launch phase at this lower gradient. The transverse laser spot on the cathode is chosen to minimize the transverse emittance and at the same time the image charge effects resulting from large charge densities at the cathode which induce an asymmetry in the longitudinal expansion and degradation of beam quality.

The shortest bunch durations (rms) obtained with this simulation study (without solenoid B) are 16.3 fs, 17.5 fs, and 18.2 fs for targets at 3.8 m, 3.0 m, and 2.5 m, respectively (Fig. 2), indicating that the reachable minimum bunch duration is relatively insensitive to the position of the focus. The longer drift length is preferred as the longitudinal focus is the shallowest. This feature relaxes the required stability of the rf phase of linac, as well as the accurate positioning of the target.

To measure a rms bunch temporal length of 16 fs level for beams of few MeVs there is no effective method currently available. Besides the ultrashort bunch length, there are also other challenges for the measurement due to the properties of the bunch generated by velocity bunching. In our scheme, (i) the charge of the bunch is restricted to 1–2 pC level to alleviate space charge effects, and (ii) the ultrashort bunch length only occurs over a short distance. Even for the 3.8 m case the bunch length grows 1.5 times larger than the minimal value for a distance of 15 cm from the longitudinal focus, shown in Fig. 2. The narrow range of compression (and the very high temporal resolution demanded to resolve the bunch) is unfavorable for employing the 9-cell X-band rf deflecting cavity available at Pegasus [36]. The weak radiation signal due to the low beam charge also makes challenging CTR-based detection schemes, imposing the use of a very sensitive bolometer detector.

TABLE I. Pegasus beam line velocity bunching parameters for 2 pC beam charge case.

Parameter	Value
Laser pulse duration	50 fs (rms)
Laser spot size on cathode	80 μm (rms)
Peak field on cathode	70 MV/m
Phase of rf gun	25 degree
Thermal emittance(per rms laser size)	0.8 mm-mrad/mm
Peak field in linac	24 MV/m
Charge	2 pC

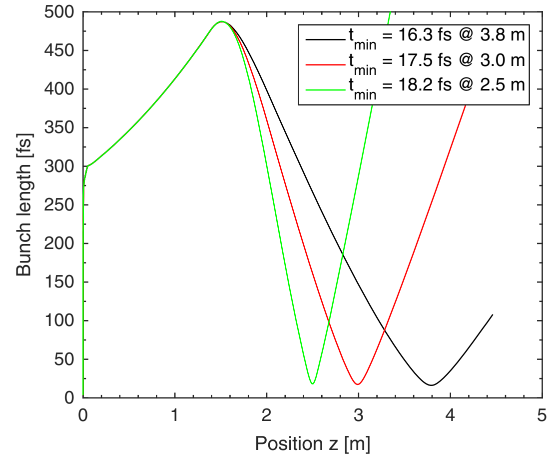

FIG. 2. The evolution of bunch length for different compression location in the velocity bunching scheme with parameters in Table I. The linac phase are −77°, −85°, −92° for bunch compression at 3.8 m, 3.0 m, and 2.5 m, respectively.

B. Modified velocity bunching scheme for CTR measurement

In our measurement setup, a high flatness gold mirror oriented at 45 degrees with respect to the beam line is installed at the longitudinal focus in the beam line to generate CTR. For reasons that will be discussed in detail in Sec. III it is very important to control the spot size at the CTR screen. We thus installed a second solenoid (solenoid B) 20 cm before the CTR target (shown in Fig. 1). During the experiment, the strength of the second solenoid (Solenoid B) is tuned to minimize the transverse spot size of the beam at the CTR target. This has an effect on the longitudinal compression dynamics as can be seen in the evolution of the rms longitudinal and transverse beam sizes for the two cases of solenoid on and off shown in Fig. 3.

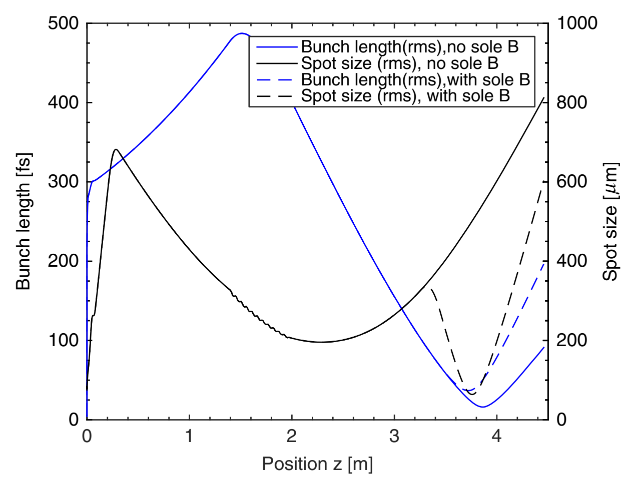

FIG. 3. The evolutions of bunch length and transverse beam size in the velocity bunching scheme with and without solenoid focusing before CTR target.

After tuning the linac phase and the strength of the solenoid B, a minimal bunch duration of 35 fs (rms) with minimal transverse spot size of 65 microns is obtained at the CTR target ($z = 3.78$ m in Fig. 3). Note that this value is larger by more than a factor of two compared to the value without any focusing. A fully 3-dimensional focus with very high charge density is obtained at the CTR target in this case. There is an obvious trade off between transverse focusing and longitudinal compression. Although at the cost of longer bunch length, the transverse focusing is indispensable in the measurement. The reason is that a small transverse beam size is required to improve the transverse coherence and thus the amount of radiation emitted, increasing the signal-to-noise ratio in the measurement. However, it should be kept in mind that the reason for introducing the transverse focusing is for CTR generation and measurement, but not for obtaining ultrashort bunch length and thus a much shorter bunch length can be generated using the velocity bunching scheme. When in the diffraction application, the solenoid B can be turned off (or set to a much lower current depending on the required spot size at the sample) without changing any other operation parameter.

C. Requirement on the charge of bunch

The most straightforward method to obtain shorter bunch is to decrease the charge of the bunch. But the charge of 2 pC used in the simulation is near the limit to generate distinguishable high frequency CTR under practical detection efficiency. For single shot electron diffraction application a charge of 1 pC is typically required [5]. It should be noted that the pC level charge is already two orders smaller than conventional CTR based measurement [25,37].

III. CTR METHOD DESCRIPTION

A. CTR calculation considering transverse coherence

In order to estimate the bunch length by characterizing the spectral content of the CTR radiation generated by the beam, it is important to understand the role played by the different beam parameters in the final radiation spectrum. A brief description of the CTR theory is reviewed here.

The CTR is generated when electron transverse a boundary between mediums of different dielectric properties, usually the vacuum and the perfect conducting surface in the experiment. The radiation generation can also be modeled as the collision of the electron with its image charge. For the 45 degree oriented mirror, the emitted radiation direction is perpendicular to the beam line, in a conelike shape in the space. With the assumption of infinite size target, infinite thin, perfectly conducting flat boundary and far-field approximation, the spectrum and spatial energy distribution of the transition radiation can be calculated analytically by Ginzburg-Frank formula [38] as:

$$\frac{\mathrm{d}^2 I_e}{\mathrm{d}\omega d\Omega} = \frac{e^2}{4\pi^3 \varepsilon_0 c}\left(\frac{\vec{\beta}\times\hat{n}}{1-\hat{n}\cdot\vec{\beta}} - \frac{\vec{\beta}'\times\hat{n}}{1-\hat{n}\cdot\vec{\beta}'}\right)^2, \tag{1}$$

where $\vec{\beta}$ and $\vec{\beta}'$ are the normalized velocity of the electrons and its image charge, $\hat{n}$ points to the observer, ω is the angular frequency, Ω is the solid angle, e is the charge of electron and ε_0 is the permittivity of vacuum.

The opening angle of the radiation cone can be derived for the single electron transition radiation (incoherent transition radiation) [39] as:

$$\theta_{\max} \approx \frac{1}{\gamma}. \tag{2}$$

Equation (2) shows for bunch of lower kinetic energy ($\gamma \sim 10$ here), the transition radiation spreads over a larger cone, requiring some care in the design of the collection optical system.

The total energy of CTR can be calculated by combining three factors: (i) the number of electrons in the bunch N, (ii) the radiation emitted by a single electron described above I_e, and (iii) the form factor containing phase information $f(\omega)$, written as:

$$\frac{\mathrm{d}I_{\mathrm{CTR}}}{\mathrm{d}\omega} = I_{\mathrm{e}}[N + N(N-1)f(\omega)]. \tag{3}$$

The form factor $f(\omega)$ is defined as the Fourier transform of the electron beam spatial distribution. The form factor can be written as:

$$f(\omega,\hat{n}) = \left|\frac{1}{N}\sum_{s=1}^{N}\exp\left(\frac{i\omega\vec{r}_s\cdot\hat{n}}{c}\right)\right|^2, \tag{4}$$

where $\vec{r}_s$ is the spatial coordinate of electron s. For the high energy case where $\hat{n}$ is confined in a cone of very small angle θ or for the case where the longitudinal dimension is much larger than the transverse one, the transverse coordinate can be neglected and Eq. (4) reduces to:

$$f(\omega) = \left|\frac{1}{N}\sum_{s=1}^{N}\exp\left(\frac{i\omega z_s}{c}\right)\right|^2. \tag{5}$$

The key point here is to observe that in the low energy case, the transverse coordinate may contribute a significant phase component to the form factor and cannot be neglected. We can decompose the $\vec{r}_s\cdot\hat{n}$ into:

$$\vec{r}_s\cdot\hat{n} = \vec{r}_T\cdot\hat{n} + \vec{r}_L\cdot\hat{n}, \tag{6}$$

where the subscripts denote the transverse and longitudinal projection, respectively. A cartoon shows the contribution from transverse (the yellow vector) and longitudinal (the red vector) dimensions in Fig. 4. Assuming a numerical

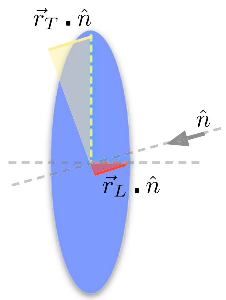

FIG. 4. Schematic of the transverse and longitudinal contributing to the coherence form factor.

case of $\gamma = 10$, transverse beam size $\sigma_x = 50\ \mu$m, bunch duration $\sigma_z = 50$ fs ($\sim$15 μm for relativistic bunch), $\theta = 20°$, the transverse beam size contribution to the form factor is 120% of the bunch length term.

B. Relative weighting of CTR spectrum using filters

To characterize the CTR spectrum in a robust way, as described in detail in the experimental section, we use two radiation filters at different wavelength (a high frequency filter centered at 61.4 μm and a low frequency filter centered at 450 μm) to select two different components of CTR which from now on we refer to as LF (low frequency) and HF (high frequency). The bandwidth and the peak transmissivity of the filters are listed in Table II. The total energy collected can be written as:

$$I_{\text{filtered}} = \int g_{\text{filter}} d\omega \int \frac{d^2 I_{\text{CTR}}}{d\Omega d\omega} d\Omega, \tag{7}$$

where the g_{filter} is the transmission function of the filter. Using the filter parameters and assuming a Gaussian shape for the transverse and longitudinal beam distributions at the CTR target, we can calculate the filtered energy as a function of the transverse size and the bunch length, shown in Fig. 5. The charge used in Fig. 5 is 1 pC.

Figure 5 shows that for the LF filter case, the radiation signal remains nearly constant for all parameter range considered. This characteristic implies the low frequency component of CTR can be used as a benchmark and calibration for the high frequency component. Conversely the energy selected by the high frequency filter is extremely sensitive to the bunch length, as well as to the transverse spot size. As the beam dimensions (either transverse or longitudinal) decrease, the high frequency components of the CTR spectrum increase significantly and the HF filtered energy can be even larger than the LF component. The ratio of the energies in the case of the two filters can be used as a good indicator of the bunch length provided the transverse beam size is known. Incidentally, Fig. 5 also shows that in order to obtain as large as possible HF CTR signal, the transverse bunch size at CTR target should be made as small as possible. This is the reason why a solenoid (the Solenoid B) before the CTR target is indispensable for the measurement.

Figure 6 shows the ratio of the HF energy over the LF energy calculated in Fig. 5 under different transverse spot sizes and bunch lengths. This quantity is independent on the beam charge and is only determined by the bunch distribution. If the transverse size of the bunch (the x coordinate) can be measured, then the bunch length (the y coordinate) can be derived from the measured CTR ratio (the contour line). It should be noted that the ratio in Fig. 6

TABLE II. Parameters of CTR filters.

	Low f filter (LF)	High f filter (HF)
Center wavelength λ_c	450 μm	61.4 μm
Bandwidth	63 μm	11 μm
Peak transmissivity	0.78	0.85
Shape	Gaussian	Gaussian

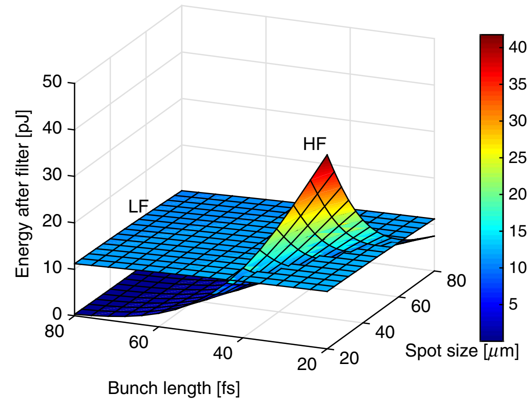

FIG. 5. Filtered energy for different bunch size (σ_x, rms) and bunch length (σ_t, rms). The HF and LF denotes the energy after high frequency filter and low frequency filter, respectively. The charge is 1 pC.

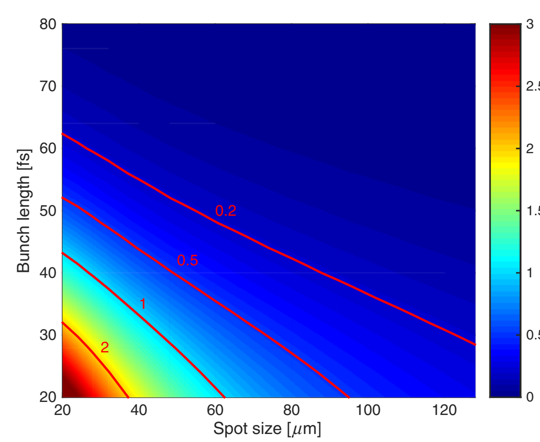

FIG. 6. The ratio of the energies of the CTR HF over LF. The color denotes the ratio value and the red solid line denotes the contour plot.

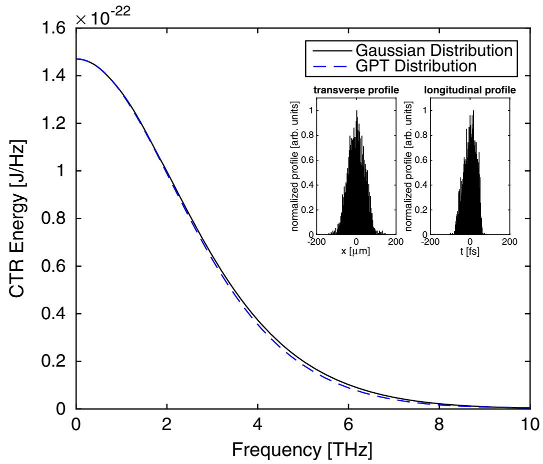

FIG. 7. The energy spectrum calculated from Gaussian distribution and the GPT simulation distribution. In the inset, we show the transverse and longitudinal profiles of the bunch.

is calculated based on the assumption of longitudinal and transverse Gaussian profile. In our particular experiment the profile (shown in Fig. 7) is somewhat different than an ideal Gaussian as it results from the space charge driven expansion of the beam in the blowout regime and resembles more a uniformly filled ellipsoidal distribution [40]. Nevertheless we calculated the ratio of the CTR energies for the two bands using the longitudinal profile obtained from GPT simulations of the bunch evolution starting from the cathode and found relatively small differences $<10\%$ for the low charges (1–10 pC) used in the experiment.

IV. EXPERIMENT RESULT AND DISCUSSION

A. CTR detection setup

The CTR collection and detection setup is shown in Fig. 8. The CTR target is a 10 mm × 10 mm square high-flatness gold mirror. To measure the transverse beam size at the CTR target plane, an imaging setup consisting of a 30 μm thick YAG screen and a 45° oriented mirror was installed. Both the CTR target and the imaging setup are mounted on a translation stage, offering the possibility to quickly switch between the CTR energy or the transverse size measurement. An off-axis parabolic mirror (OAP1) is installed with the focal point at the CTR target to collimate the radiation. The collection efficiency of the parabolic mirror is $>85\%$ for the calculated spatial distribution of the CTR. Two THz mirrors and a second OAP (OAP2) are used to guide the CTR through a high-transmissivity polymethylpentene TPX window commercially available from Tydex out of the vacuum chamber and a THz filter wheel outside the chamber. For detection we used a high-sensitivity (2.73×10^5 V/W), liquid He cooled bolometer from IRLabs.

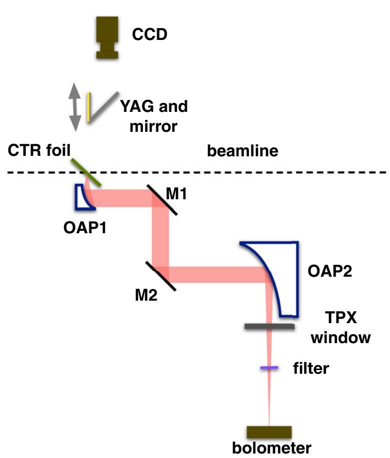

FIG. 8. The schematic of the CTR collection setup.

B. Experiment data

In the experiment, we tune iteratively the phase of linac and the strength of the solenoid to optimize the CTR signal. The linac phase is first set at the value indicated by the GPT simulation, and then the strength of the solenoid is tuned to minimize the transverse beam size. Then the YAG is replaced with the CTR target and the high frequency CTR energy signal is again maximized using the linac phase. According to the simulation, the maximum high frequency CTR energy can be obtained when the local minimal transverse spot size and the local shortest bunch length both locate at the CTR target. After several iteration rounds, the optimum parameters set can be determined and then the detected energy after both filters are recorded and fitted. The detector response is assumed to be flat in the region of interest, but in the calibration of the signals we take into account the transmission of the vacuum window which is 85% and 67% for 450 μm and 61.5 μm, respectively and the transmission of the bolometer window (93% at 450 μm and 80% at 61.5 μm).

The averaged measured high frequency and the low frequency energy are shown in Fig. 9, for various beam

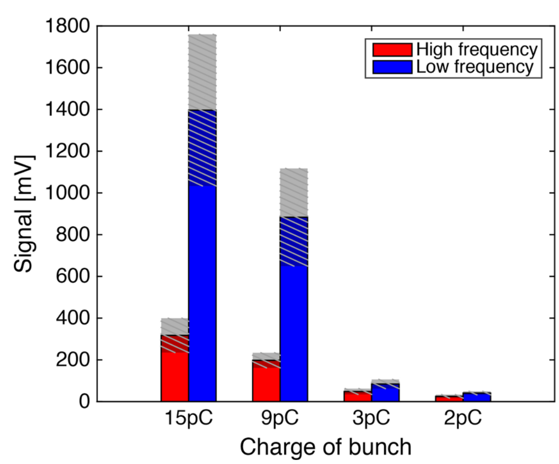

FIG. 9. The measured bolometer signal with low frequency filter and high frequency filter under different charges. The shaded area denotes the standard error.

charges, namely 2 pC, 3 pC, 9 pC, and 15 pC. An obvious trend can be found that as the charge decreases, the level of LF CTR signal catches up with the HF level, confirming as predicted by simulations a decrease in the bunch dimensions and a consequent coherent enhancement. For each beam charge, the transverse spot size is also measured and agrees well with simulation results, as shown in Fig. 10.

For the measured CTR energy, the shot-to-shot rms fluctuations are typically between 20%–30% (shown as the shaded area in Fig. 9). These large fluctuations of signals are due to several sources. The jitter in rf amplitude and phase, and the pointing fluctuations of the laser all cause the maximum compression and focus point to shift from the CTR target location, resulting in a reduction of the coherent form factor and thus in the energy of high frequency component. According to simulations, we estimate for the HF signal a variation of about 10% for each degree of phase jitter for the 2 pC case. Furthermore, a shift in the injection phase will also contribute to amplify the jitter in photo-emitted charge due to the Schottky effect at the cathode. Added to the 15% fluctuations in the photocathode drive lasers, this results in large shot-to-shot fluctuations of the beam charge as indicated by the jitter in the low frequency component of the signal. Note that the bolometer signals recorded by the oscilloscope are several times larger than the noise floor level which is less than 1 mV, therefore the detector cannot be considered a major sources of the jitter.

Before using the measured signal to derive the bunch length according the method described above, we note that the HF over LF ratio obtained in Fig. 6 is based on the assumption of ideal THz filter with zero transmission outside the pass band. However, in the experiment, this assumption is not fully satisfied and the background originating from the frequency components lying outside the HF filter bandpass must be taken into account. In fact, for the high charge case of 15 pC the CTR spectrum should have little contribution (~3 percent) to the HF signal and the measured radiation are background due to frequency components leaking through the filter. We use the measurement under 15 pC and determine the background factor as 1.75%, which is consistent with the filter specifications indicated value of 2% transmission over the entire signal bandwidth outside the bandpass.

Conversely, in the CTR spectrum emitted by the ultrashort bunches at low charges (2 pC and 3 pC) the high frequency component is dominant over the background. To give an idea of the uncertainty introduced by the background in the measurement, a 10% error in determining the background coefficient would result in less than 5% error in the high frequency CTR energy at 2 pC.

In Fig. 11, we use the detector calibration and the transmission of the optical transport system to derive the energies measured in the high frequency and low frequency bands in the CTR spectrum as a function of charge. The background is subtracted using a factor of 1.75% for HF signal under each charge. The low frequency CTR energy is proportional to the square of the beam charge (as it should be) and consistent with simulations.

The large error bars are due to the large fluctuations observed in the signals (see Fig. 8 shaded areas). The rms fluctuations of the CTR signals are as large as 25%, which propagates to a 50% error in their ratio. The derived HF/LF ratios are 0.31 ± 0.15, 0.32 ± 0.15, 0.05 ± 0.025 for 2 pC, 3 pC, and 9 pC beam charges, respectively. Taking into account the transverse spot size from Fig. 9, we can derive the bunch lengths which are summarized in Table III.

As shown in Table III, we estimate for the 2 pC bunch with pulse duration of 42 fs $\pm$ 9 fs, which agrees with the simulation result of 35 fs. For the 3 pC bunch, the derived bunch length is 32 ± 13 fs also in agreement with the simulation which indicates a 43 fs bunch length. The derived 3 pC charge is shorter than the 2 pC, which is surprising but still consistent considering the large fluctuation of CTR and unstable spot size under 3 pC. For the 9 pC bunch, the derived bunch length is 56 ± 6 fs, not

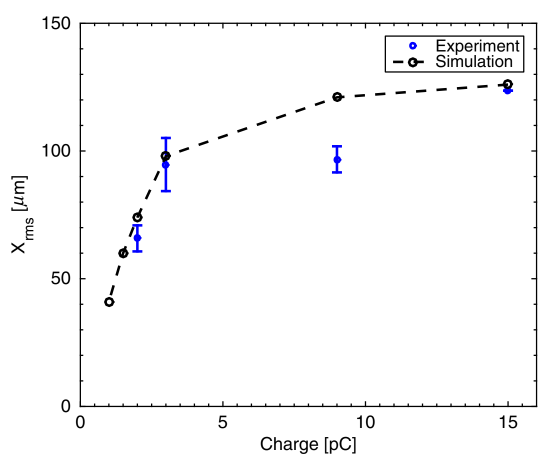

FIG. 10. Measured rms transverse spot size for different charges Q, compared with simulation from GPT.

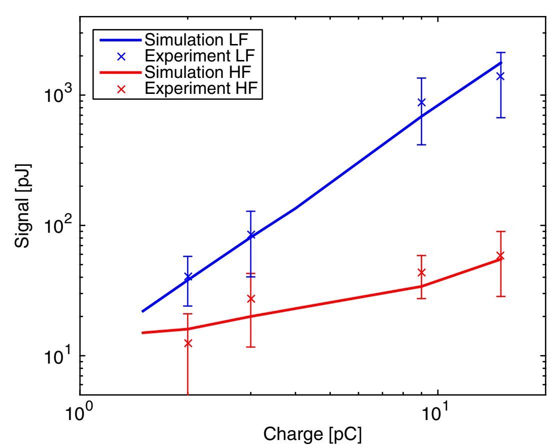

FIG. 11. The simulated energy and the experimental energy (background subtracted) of LF and HF filtered CTR for different beam charges Q.

TABLE III. Measured electron pulse duration.

Charge	Bunch length	Simulation
2 pC	33 fs–51 fs	35 fs
3 pC	18 fs–44 fs	38 fs
9 pC	50 fs–63 fs	71 fs

very consistent with simulation and may due to large background signal and inconsistent spot size measurement (see Fig. 10). The 15 pC case is not shown in Table III because it is used for calibration the background factor.

As discussed in the previous sections, when the second focusing is turned off, the bunch length is expected to be half of the measured value, or about 16 fs as indicated by the simulation. When the charge is decreased further, even shorter bunch length is expected to be obtained. However in that case the CTR radiation becomes too weak to be detected using the bolometer after the filters. For beams of different bunch lengths, proper filter pairs or more filters can be used to improve the method.

V. CONCLUSION

In summary, we have studied the velocity compression of a beam generated from a rf photoinjector operating in the blowout regime. A simplified CTR-spectrum based method is developed to measure ultrashort bunch of length shorter than 50 fs in presence of several constraints (few MeV beam energy, below 2 pC beam charge and tight longitudinal focus) which would make all other conventional longitudinal diagnostics unsuitable for this problem. The effect of the transverse focusing before CTR target is discussed. The transverse coherent effect is found to be significant and should be taken into consideration when calculating the CTR spectrum from the beam parameters. The ratio of high frequency and low frequency components can be used to obtain an estimate on the bunch length. The experiment shows a minimum electron pulse duration shorter than 40 fs (rms) for 2 pC in agreement with simulation results. The results reported here suffer from the large fluctuations of the beam parameters during the multi-shot measurement technique. This is not a fundamental limitation of the velocity compression scheme, since much better reliability and stability of the system have been demonstrated elsewhere [41,42], nevertheless it points out that achieving ultrashort pulse durations is deeply linked to the progress in the stability of the rf and laser system. In applications where tight focusing of the beam is not required, the same simulation model yields a pulse duration as short as 16 fs, since the space charge effect on bunch lengthening is much alleviated compared to the 3-dimensional focused and compressed case. These results are a first step in the application of rf compression methods to relativistic beams and indicate a path toward 10 fs temporal resolution in ultrafast electron diffraction techniques.

ACKNOWLEDGEMENTS

This work was supported by DOE Grant No. DE-FG02-92ER40693, NSF award No. PHY 1415583 and National Natural Science Foundation of China (Grant No. 11127507, and Grant No. 10925523).

[1] A. H. Lumpkin, R. Dejus, W. J. Berg, M. Borland, Y. C. Chae, E. Moog, N. S. Sereno, and B. X. Yang, Phys. Rev. Lett. **86**, 79 (2001).

[2] J. Faure, C. Rechatin, A. Norlin, A. Lifschitz, Y. Glinec, and V. Malka, Nature (London) **444**, 737 (2006).

[3] Y. Shen, T. Watanabe, D. A. Arena, C.-C. Kao, J. B. Murphy, T. Y. Tsang, X. J. Wang, and G. L. Carr, Phys. Rev. Lett. **99**, 043901 (2007).

[4] A. H. Zewail, Annu. Rev. Phys. Chem. **57**, 65 (2006), pMID: 16599805, http://dx.doi.org/10.1146/annurev.physchem.57.032905.104748.

[5] G. Sciaini and R. J. D. Miller, Rep. Prog. Phys. **74**, 096101 (2011).

[6] B. E. Carlsten and S. J. Russell, Phys. Rev. E **53**, R2072 (1996).

[7] S. G. Anderson, P. Musumeci, J. B. Rosenzweig, W. J. Brown, R. J. England, M. Ferrario, J. S. Jacob, M. C. Thompson, G. Travish, A. M. Tremaine, and R. Yoder, Phys. Rev. ST Accel. Beams **8**, 014401 (2005).

[8] M. Ferrario *et al.*, Phys. Rev. Lett. **104**, 054801 (2010).

[9] P. Musumeci, J. T. Moody, C. M. Scoby, M. S. Gutierrez, and M. Westfall, Appl. Phys. Lett. **97**, 063502 (2010).

[10] R. Li, C. Tang, Y. Du, W. Huang, Q. Du, J. Shi, L. Yan, and X. Wang, Rev. Sci. Instrum. **80**, 083303 (2009).

[11] X. Wang, D. Xiang, T. Kim, and H. Ihee, J. Korean Phys. Soc. **48** (2006).

[12] X. J. Wang, X. Qiu, and I. Ben-Zvi, Phys. Rev. E **54**, R3121 (1996).

[13] P. Musumeci, L. Faillace, A. Fukasawa, J. Moody, B. O'Shea, J. Rosenzweig, and C. Scoby, Microsc. Microanal. **15**, 290 (2009).

[14] A. Fukasawa (to be published).

[15] O. J. Luiten, S. B. van der Geer, M. J. de Loos, F. B. Kiewiet, and M. J. van der Wiel, Phys. Rev. Lett. **93**, 094802 (2004).

[16] P. Musumeci, J. T. Moody, R. J. England, J. B. Rosenzweig, and T. Tran, Phys. Rev. Lett. **100**, 244801 (2008).

[17] K. Floettmann, Nucl. Instrum. Methods Phys. Res., Sect. A **740**, 34 (2014); in *Proceedings of the First European Advanced Accelerator Concepts Workshop 2013, La Biodola, Isola d'Elba, 2013*.

[18] R. Akre, L. Bentson, P. Emma, and P. Krejcik, in *Proceedings of the Particle Accelerator Conference, Chicago, IL, 2001* (IEEE, New York, 2001).

[19] D. Alesini and F. Marcellini, Phys. Rev. ST Accel. Beams **12**, 031301 (2009).

[20] G. Berden, S. P. Jamison, A. M. MacLeod, W. A. Gillespie, B. Redlich, and A. F. G. van der Meer, Phys. Rev. Lett. **93**, 114802 (2004).

[21] G. Berden, W. A. Gillespie, S. P. Jamison, E.-A. Knabbe, A. M. MacLeod, A. F. G. van der Meer, P. J. Phillips,

H. Schlarb, B. Schmidt, P. Schmüser, and B. Steffen, Phys. Rev. Lett. **99**, 164801 (2007).

[22] Y. Glinec, J. Faure, A. Norlin, A. Pukhov, and V. Malka, Phys. Rev. Lett. **98**, 194801 (2007).

[23] A. Tremaine, J. B. Rosenzweig, S. Anderson, P. Frigola, M. Hogan, A. Murokh, C. Pellegrini, D. C. Nguyen, and R. L. Sheffield, Phys. Rev. Lett. **81**, 5816 (1998).

[24] M. Ding, H. Weits, and D. Oepts, Nucl. Instrum. Methods Phys. Res., Sect. A **393**, 504 (1997); in *Proceedings of 18th International FEL Conference and Users Workshop, Rome, Italy, 1996 (1996).*

[25] A. Murokh, J. Rosenzweig, M. Hogan, H. Suk, G. Travish, and U. Happek, Nucl. Instrum. Methods Phys. Res., Sect. A **410**, 452 (1998).

[26] S. Wesch, B. Schmidt, C. Behrens, H. Delsim-Hashemi, and P. Schmser, Nucl. Instrum. Methods Phys. Res., Sect. A **665**, 40 (2011).

[27] R. Lai, U. Happek, and A. J. Sievers, Phys. Rev. E **50**, R4294 (1994).

[28] S. I. Bajlekov, M. Heigoldt, A. Popp, J. Wenz, K. Khrennikov, S. Karsch, and S. M. Hooker, Phys. Rev. ST Accel. Beams **16**, 040701 (2013).

[29] A. H. Lumpkin, N. S. Sereno, W. J. Berg, M. Borland, Y. Li, and S. J. Pasky, Phys. Rev. ST Accel. Beams **12**, 080702 (2009).

[30] T. van Oudheusden, P. L. E. M. Pasmans, S. B. van der Geer, M. J. de Loos, M. J. van der Wiel, and O. J. Luiten, Phys. Rev. Lett. **105**, 264801 (2010).

[31] S. Tokita, K. Otani, T. Nishoji, S. Inoue, M. Hashida, and S. Sakabe, Phys. Rev. Lett. **106**, 255001 (2011).

[32] R. K. Li, P. Musumeci, H. A. Bender, N. S. Wilcox, and M. Wu, J. Appl. Phys. **110**, 074512 (2011).

[33] J. T. Moody, P. Musumeci, M. S. Gutierrez, J. B. Rosenzweig, and C. M. Scoby, Phys. Rev. ST Accel. Beams **12**, 070704 (2009).

[34] D. J. Newsham, N. Barov, and R. H. Miller, *Proceedings of the 24th Particle Accelerator Conference, PAC-2011, New York, 2011* (IEEE, New York, 2011), p. 1897.

[35] Pulsar Physics, http://www.pulsar.nl/gpt.

[36] P. Musumeci, J. T. Moody, C. M. Scoby, M. S. Gutierrez, M. Westfall, and R. K. Li, J. Appl. Phys. **108**, 114513 (2010).

[37] D. Mihalcea, C. L. Bohn, U. Happek, and P. Piot, Phys. Rev. ST Accel. Beams **9**, 082801 (2006).

[38] V. L. Ginzburg and I. M. Frank, *Sov. Phys. JETP* ***16**, 15 (1946)*.

[39] A. M. Tremaine, Ph.D. thesis, University of California, Los Angeles, 1999.

[40] W. P. E. M. Op 't Root, P. W. Smorenburg, T. van Oudheusden, M. J. van der Wiel, and O. J. Luiten, Phys. Rev. ST Accel. Beams **10**, 012802 (2007).

[41] R. Akre, D. Dowell, P. Emma, J. Frisch, S. Gilevich, G. Hays, P. Hering, R. Iverson, C. Limborg-Deprey, H. Loos, A. Miahnahri, J. Schmerge, J. Turner, J. Welch, W. White, and J. Wu, Phys. Rev. ST Accel. Beams **11**, 030703 (2008).

[42] F. Stephan *et al.*, Phys. Rev. ST Accel. Beams **13**, 020704 (2010).